Gynecologic Oncology 152 (2019) 166–176

Contents lists available at ScienceDirect

Gynecologic Oncology

journal homepage: www.elsevier.com/locate/ygyno

Effect of lamin-A expression on migration and nuclear stability of ovarian cancer cells

Yixuan Wang [a,b], Jing Jiang [b], Liuqing He [b], Guanghui Gong [a,b], Xiaoying Wu [a,b,*]

[a] Department of Pathology, Xiangya Hospital, Central South University, Changsha, Hunan, China
[b] Department of Pathology, School of Basic Medical Science, Central South University, Changsha, Hunan, China

HIGHLIGHTS

- Lamin-A was critical for cells passing through pores and survival.
- Lamin-A knockdown could enhance migration ability, while overexpression could weaken the capacity to migrate.
- Lamin-A knockdown increased nuclear plasticity, and the morphology was easier to recover after migration.
- When lamin-A was further knockdown, cells migrated through restricted pores decreased unexpectedly, with severe DNA damage.
- BRCA1, Ku80 and Rad50 were down-regulated after lamin-A further knockdown, suggesting DNA repair pathways were impaired.

GRAPHICAL ABSTRACT

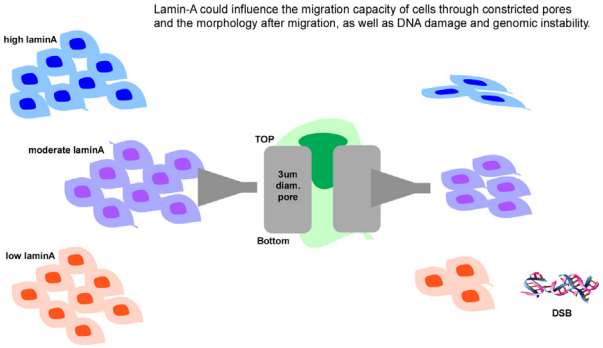

ARTICLE INFO

Article history:
Received 8 August 2018
Received in revised form 18 October 2018
Accepted 22 October 2018
Available online 29 October 2018

Keywords:
Lamin-A
Ovarian cancer
Migration
Nucleus
DNA damage

ABSTRACT

Objective. Nuclear lamina plays important roles in nuclear shape and mechanical stability. Many studies demonstrated that defects of lamin-A were associated with several diseases, but little research was found on its potential roles in ovarian cancer.

Methods. GEPIA and GEO database were used to analyze lamin-A in ovarian tissues, followed by assessing lamin-A and prognosis of ovarian cancer patients with Kaplan-Meier plotter. Then, transient transfected HO-8910 cells with shRNA to knockdown lamin-A. Knockdown efficiency was determined by western blot, qRT-PCR and immunofluorescence. Meanwhile, lamin-A was overexpressed in HO-8910 PM cells. Then, 2D migration, 3D migration through 3 μm and 8 μm pores were carried out, followed by immunofluorescence and TEM observation.

Results. Lamin-A tended to be lower in ovarian cancer, and higher expression of lamin-A was associated with better survival. After lamin-A knockdown, 2D and 3D migration (3 μm, 8 μm) abilities of HO-8910 cells were significantly increased ($p < 0.001$), while overexpression of lamin-A in HO-8910PM impeded migration. Meanwhile, when HO-8910 cells migrated through 3 μm pores, nuclei became strikingly elongated, and down-regulation of lamin-A promoted nuclear plasticity, making the circularity of nucleus increased. Besides, further knockdown group had the highest proportion of γ-H2AX, with micronuclei forming. Furthermore, western blot showed that the expression of BRCA1, Ku80 and Rad50 decreased significantly after further knockdown, suggesting impairment of DNA damage repair.

Conclusions. Lamin-A was down-regulated in ovarian cancer, and higher lamin-A was associated with better prognosis. Nuclei with high lamin-A were severely deformed through constricted pores. Moderate lamin-A

* Corresponding author at: Department of Pathology, Xiangya Hospital, Central South University, Changsha 410008, China.
E-mail address: xyw2007@csu.edu.cn (X. Wu).

https://doi.org/10.1016/j.ygyno.2018.10.030

enhanced nuclear plasticity, so as to strengthen migration ability. When lamin-A was further knockdown, ovarian cancer cells that migrated through restricted pores decreased, with DNA damage, genomic instability and impairment of DNA damage repair.

1. Introduction

Nuclear lamins are the main components of the nuclear lamina, which generally exist in eukaryotic cells. Lamins interact with membrane-associated proteins to form the nuclear lamina, and are closely related to nuclear membrane, chromatin and nuclear pore complex. The nuclear lamina is found between the inner nuclear membrane and the peripheral chromatin. It plays an important role in the breakdown and reformation of the nuclear envelope during cell division. Lamins can be divided into A and B type, encoded by three distinct genes, LMNA, LMNB1 and LMNB2 [1]. Normally, LMNA gene can encode four A type lamins (A、A△lO、C、C2), they are all derived from LMNA through alternative splicing. Among them, A and C are the major parts. As central components of nuclei, they can influence nuclear shape and stability, and are required for mechanical stability, chromatin organization, gene regulation, nuclear positioning and cell division [2].

The LMNA gene locates at chromosome 1q21.1–21.3, and encodes for lamin-A and lamin-C protein, which are major components of the nuclear lamina [1]. The mutation of LMNA gene could increase the content of the nuclear lamina binding to the telomere, changing the location of telomere. Telomere is closely related to cell life, so the mutation of LMMA often affects the lifetime of cells. Many studies have demonstrated that mutations in the LMNA gene or defects of lamin-A were associated with several diseases including E familial partial lipodystrophy, mery-Dreifuss muscular dystrophy, dilated cardiomyopathy and Hutchinson–Gilford progeria syndrome [3,4].

Ovarian cancer is the most malignant gynecologic malignancy, and is prone to invasion, metastasis and recurrence. The majority of patients have no obvious symptoms and are diagnosed late-stage ovarian cancer, with distant metastasis occurred. But the molecular mechanisms underlying metastasis is poorly understood. Previous studies have demonstrated that lamin-A levels could change in many diseases, and could vary greatly depending on the subtypes and characteristics of tumor cells. Down-regulation of lamin-A has been shown in several tumor types such as gastric carcinoma [5], and was also correlated with the poor prognosis of primary gastric carcinoma and colon cancer [5,6]. Besides, lamin-A was also related to the recurrence and aberrant nuclear morphology of ovarian cancer and breast cancer [7,8]. On the contrary, researchers also discovered that lamin-A was a potential colorectal cancer biomarker [9], indicating a more aggressive phenotype and a worse prognosis with high levels. However, little research was found on the potential roles of lamin-A in ovarian cancer. Our previous studies have demonstrated that VEGF could promote the invasion of ovarian cancer partially via down-regulation of Ezrin and Lamin-A/C, caused by the increase of miR-205 [10]. Further studies confirmed that it was lamin-A that decreased, lamin-C did not change significantly [11]. Therefore, the aim of our study is to investigate the effects of lamin-A on the migration of ovarian cancer, and its potential role in the nuclear stability of ovarian cancer cells.

2. Methods

2.1. Cell lines and cell culture

HO-8910 and HO-8910PM are two kinds of human ovarian cancer cell lines. HO-8910PM is a highly metastatic cell line derived from HO-8910. HO-8910 cells were purchased from CCTCC (China Center for Type Culture Collection, Wuhan, China). HO-8910PM cells were kindly donated by Professor Xin Lu (Obstetrics and Gynecology Hospital, Fudan University, Shanghai, China). All cells were cultured using standard protocols. HO-8910PM cells were cultured in DMEM high-glucose Media, HO-8910 cells were cultured in RPMI-1640 media (BI, Biological Industries), supplemented with 10% fetal bovine serum (BI, Biological Industries). All cells were maintained at 37 °C under 5% CO_2.

2.2. Lamin-A knockdown

All GFP–shRNAs were purchased from GENECHEM (Shanghai, China). Before transfection, HO-8910 cells were plated at 2×10^5 cells/well in 6-well cell culture plates. The transient transfection complex was prepared in Opti-MEM reduced serum medium (GIBCO, Life Technologies) following the manufacturer's instructions. A complex of 2 μg shRNA and 1 μg/ml Lipofectamine2000 4 μl was prepared. A single dose was denoted as "shRNA+" to achieve moderate knockdown, and three doses to achieve further knockdown were denoted as "shRNA+++", compared with those using the same doses of scrambled shRNA (scr shRNA). Cells were maintained at 37 °C for 6–8 h, then the medium was replaced with RPMI-1640 complete medium. Knockdown efficiency was determined by western blot, qRT-PCR and immunofluorescence staining after 24 h. Antibodies against lamin-A (mouse, ab-8980) was from Abcam, U.K.

2.3. Lamin-A overexpression

The plasmids encoding lamin-A with flag tag were purchased from GENECHEM (Shanghai, China). Cells were transfected with flag-lamin-A and the corresponding empty vector. Before transfection, cells were plated at 2×10^5 cells/well in 6-well cell culture plates. Then 2 μg plasmid and 4 μl lipofectamine2000 (Life Technologies, Carlsbad, CA) were diluted in 0.2 ml Opti-MEM medium (GIBCO, Life Technologies) following the manufacturer's instructions. Subsequently, cells were maintained at 37 °C for 6–8 h, then the mixture was replaced by 2 ml of DMEM complete culture medium. Western blot and qRT-PCR were performed after 24 h to detect the overexpression efficiency.

2.4. Migration assay

Transwell inserts with 3 μm or 8 μm pore size were purchased from Corning (Inc, NY). For migration, 10^5 cells were seeded in serum-free medium on the top well, and normal culture medium with 10% FBS was added to the bottom well. After incubation at 37 °C for 24 h, non-migrating cells in the upper chamber were removed by cotton swab, and the cells on the bottom of the filters were fixed with 4% paraformaldehyde for 30 min, then stained with 0.1% crystal violet for 20 min. The number of migrating cells was quantitated using Image-Pro plus software.

2.5. Wound healing assay

10^5 cells were seeded on 6-well cell culture plates. The next day, cells were treated with shRNA (lamin-A knockdown or scrambled). After 24 h, cells were wounded with a 20 μl sterile micropipette tips, and then washed with serum-free medium to remove detached cells. Photos were taken of the same area at 0 h, 24 h, 48 h, and 72 h to measure the width of the wound.

2.6. Quantitative RT-PCR (qRT-PCR) analysis

Total RNA was harvested using Trizol reagent (Takara, Japan), and reverse transcribed into cDNA using the GoScript Reverse Transcription (RT-PCR) System (Promega, Madison, WI, USA). Primers were synthesized by Generay Company (Shanghai, China). Quantitative RT-PCR was performed using ABI Prism 7500 system with GoTaq qPCR Master Mix (Promega, Madison, WI, USA) according to the manufacturer's instruction. GAPDH was used as an internal control.

2.7. Western blotting

Cells were lysed in lysis buffer containing protease inhibitor. Protein concentration was determined using a BCA protein assay kit (Novagen, Merck Group, Madison, USA). Equal amounts of denatured proteins were separated by SDS-PAGE gels and then transferred onto PVDF membranes (Millipore, Bedford, MA, USA). The membranes were blocked in 5% non-fat milk at room temperature for 1 h, and then incubated with primary antibody, followed by horseradish peroxidase-conjugated secondary antibody. Protein expression levels were detected using Image Lab software (Bio-Rad, CA, USA).

2.8. Immunofluorescence staining

Transwell membranes or glass slides were fixed in 4% formaldehyde for 30 min at room temperature followed by PBS washing. Then permeabilized by 0.01% TritonX-100 for 30 min, blocked by 5% BSA, and incubated in primary antibody at room temperature for 1 h, and stayed overnight at 4 °C. Finally, the primary antibody was tagged with the corresponding secondary antibody for 1 h at room temperature. Images were photographed with Olympus DP73 fluorescence microscope.

2.9. Transmission electron microscopy

Cells were detached from plates using 0.05% Trypsin-EDTA, and then collected them by 5 min of centrifugation at 1100 rpm. Fixation was performed with 2.5% glutaraldehyde at 4 °C for >24 h, and then post-fixed in 2% osmic acid, followed by dehydrated in graded acetone and embedding. Semithin sections were cut and stained with toluidine blue for light microscopy. Then, ultrathin sections were obtained with a Leica ultramicrotome, collected on copper grids and counterstained with uranyl acetate and lead nitrate for imaging. The specimens were observed by a transmission electron microscopy (TEM, HT770, Japan).

2.10. Search strategy

Microarray profiles (up to 23 September 2018) that explored lamin-A in ovarian cancer tissues and normal ovarian tissues were obtained from the Gene Expression Ominibus (GEO) database in NCBI (http://www.ncbi.nih.gov/geo), using the keywords “ovarian cancer”. Database searching was carried out by two researchers independently (Yixuan Wang and Liuqing He). The microarrays that met the following criteria were collected: (a) studies including at least 30 samples; (b) examination of mRNA expression in ovarian cancer patients' tissues and normal tissues; (c) samples containing completed data for analysis. In the initial screening, a total of 96 potentially relevant datasets were selected. After reading summary and relevant information, a total of 4 GEO datasets (GSE27651, GSE40595, GSE25427, GSE12470) were included. As the data were obtained from GEO, further approval by an ethics committee was not required.

3. Statistical analysis

All data were presented as the mean values ± the standard error of the mean from at least 3 independent experiments. Two-tailed Student's *t*-test was used for comparison between two groups. Statistical analyses were carried out using Graphpad Prism 5.0. Error bars indicate the standard deviation in all the figures. p value < 0.05 was considered statistically significant. $^{*}p < 0.05$, $^{**}p < 0.01$, $^{***}p < 0.001$.

4. Results

Lamin-A was down-regulated in ovarian cancer tissues, and higher expression of lamin-A was associated with better survival in ovarian cancer patients.

In our previous study, paraffin sections were used to detect the expression of lamin-A in ovarian tissues (61 cases of ovarian cancer, 14 cases of benign ovarian tumors and 13 cases of normal ovarian tissues) [11]. The results indicated that lamin-A expression was significantly lower in ovarian cancer than in the normal and the benign groups ($p < 0.05$) [11]. Then, lamin-A expression obtained from Gene Expression Profiling Interactive Analysis (GEPIA) online database were assessed [12]. In agreement with our previous study, lamin-A tended to be lower in many kinds of cancers including ovarian cancer (Fig. 1A). To further validate these findings, data from GEO database (GSE40595 [13], GSE25427 [14], GSE12470 [15], GSE27651 [16]) were analyzed. Results showed that expressions of lamin-A in ovarian cancer tissues were significantly lower than those in normal ovarian tissues (all $p < 0.001$), which was in accordance with our previous findings. Furthermore, lamin-A expression of high-grade ovarian cancer was lower than that in low-grade ovarian cancer (Fig. 1D).

We also assessed the association between lamin-A expression and prognosis using the Kaplan–Meier plotter database [17]. Patients with high lamin-A had significantly longer OS (overall survival) and PFS (progression free survival) than patients with low lamin-A in ovarian cancer (Fig. 1B, $p = 0.0093$; Fig. 1C, $p = 0.018$).

Moderate knockdown of lamin-A enhanced migration capacity of ovarian cancer cells.

Transient transfected HO8910 cell line with shRNA to moderate knockdown lamin-A, and total protein and RNA were extracted 24 h after transfection. Then western blot and qRT-PCR were used to detect the protein and mRNA expression changes. After transfected with shRNA, about 30%–40% lamin-A was inhibited (Supplementary Fig. S1A, Fig. 2A, $p < 0.05$). Results showed that 2D migration (wound-healing assay) rate of HO-8910 cells was accelerated after lamin-A knockdown (Supplementary Fig. S1B, $p < 0.001$). Next, 3D migration (transwell assay) was carried out through relatively large pores (8 μm), and found that the number of cells transferred through the filters increased significantly in lamin-A knockdown group than control (Supplementary Fig. S1C, $p < 0.001$), suggesting that both the 2D and 3D migration capacities of HO-8910 cells were enhanced after lamin-A knockdown.

Further knockdown of lamin-A impeded migration capacity of ovarian cancer cells through restricted pores.

After treatment of a single dose or three doses of shRNA for 24 h, western Blot, qRT-PCR and immunofluorescence were used to detect the knockdown efficiency (Fig. 2A, B). In the further knockdown group, lamin-A was inhibited about 70%–80% compared to control (Fig. 2A). Immunofluorescence staining showed a significant decline of lamin-A intensity in the further knockdown group compared with moderate knockdown (Fig. 2B, $p < 0.05$). Then, wound healing assay, transwell assay were performed to assess cell migration. The abilities of 2D migration and 3D migration through relative large pores (8 μm) were enhanced after lamin-A moderate and further knockdown, whereas no significant difference was found between them (Fig. 2C, D), indicating that the degree of knockdown could not affect the ability of 2D and 3D migration through larger pores. However, when the three groups were migrated through relative small filters (3 μm), the number of migrated cells decreased in the further knockdown group surprisingly (Fig. 2E, $p < 0.001$), which showed that further knockdown lamin-A could weaken the ability of cells passing through restricted pores (3 μm).

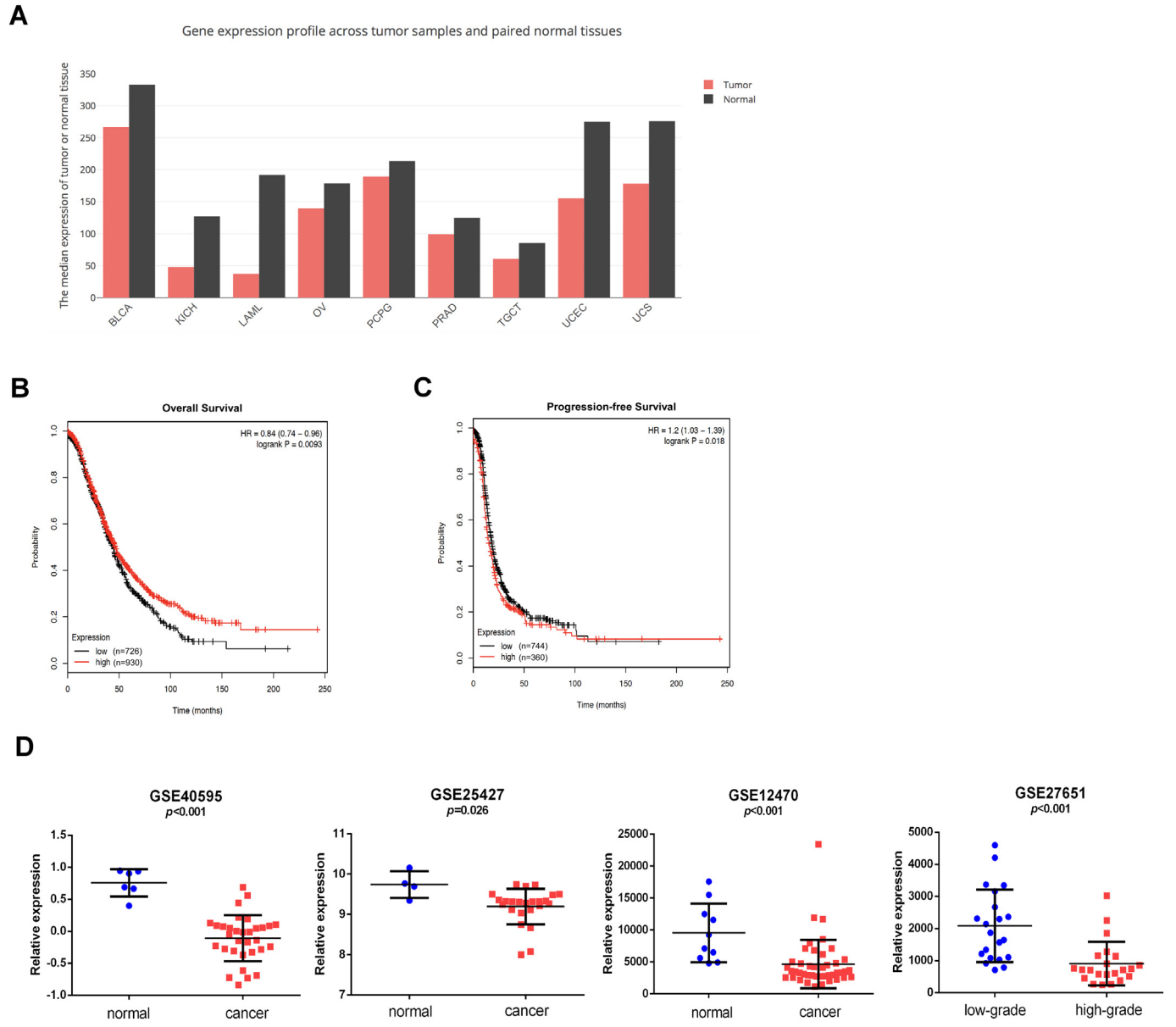

Fig. 1. Lamin-A was down-regulated in ovarian cancer tissues, and higher expression of lamin-A was associated with better survival in ovarian cancer patients. A: lamin-A expression profile across TCGA datasets. Images were taken from GEPIA online database (http://gepia.cancer-pku.cn). BLCA, Bladder Urothelial Carcinoma; KICH, Kidney Chromophobe; LAML, Acute Myeloid Leukemia; OV, Ovarian serous cystadenocarcinoma; PCPG, Pheochromocytoma and Paraganglioma; PRAD, Prostate adenocarcinoma; TGCT, Testicular Germ Cell Tumors; UCEC, Uterine Corpus Endometrial Carcinoma; UCS, Uterine Carcinosarcoma. B, C: Kaplan–Meier curves for OS (overall survival) and PFS (progression free survival) in ovarian cancer using the Kaplan–Meier Plotter database (www.kmplot.com). Red and black lines indicated patients with higher and lower than median lamin-A expression, respectively. D: Expression levels of lamin-A in ovarian tissues from GSE40595, GSE25427, GSE12470, and GSE27651 database. Normal, normal ovarian tissue; cancer, ovarian cancer tissue; low-grade, low-grade ovarian cancer; high-grade, high-grade ovarian cancer.

Lamin-A knockdown influenced the nuclear morphology, DNA damage, and micronuclei formation after migrated through constricted pores.

In assessing migration, shapes of nuclei on the bottom of the 8 μm transwell filters appeared indistinguishable from 2D cultures, regardless of lamin-A levels (Fig. 3A). But we noticed that nuclear shapes on the bottom of the 3 μm filters were strikingly elongated compared with the typical elliptical shapes on the top (Fig. 3A), and the nuclear circularity increased in cells transfected with shRNA+, and was even higher after transfected with shRNA++ (Fig. 3A). These results suggested that the nuclear morphology after constricted migration was related to lamin-A level. However, for 8 μm pores, lamin-A knockdown had no effect on shapes of nuclei on the filter bottoms. In addition, the expression of γ-H2AX (a DNA double strand break marker) was observed after migration through 3 μm pores both in lamin-A moderate knockdown group and in further knockdown group, but the positive rate of the latter was higher (Fig. 3B, $p < 0.01$), with γ-H2AX positive micronuclei formed (Fig. 3C), indicating DNA damage and genomic instability after restricted migration. On the other hand, the positive rate of γ-H2AX was extremely low after passing through larger filters (8 μm), suggesting that DNA damage was rare for cells migrating through larger pores, regardless of lamin-A level (Fig. 3D). The results suggested that DNA damage was easy to happen in cells passing through constricted pores, and damage was more serious with the decrease of lamin-A. As the repair of DNA double strand break (DSBs) is conducted via non-homologous end joining (NHEJ) and homologous recombination (HR), of which BRCA1, Ku80, Rad50 are the key proteins, so the activation of DNA damage response kinases was tested by western blot.

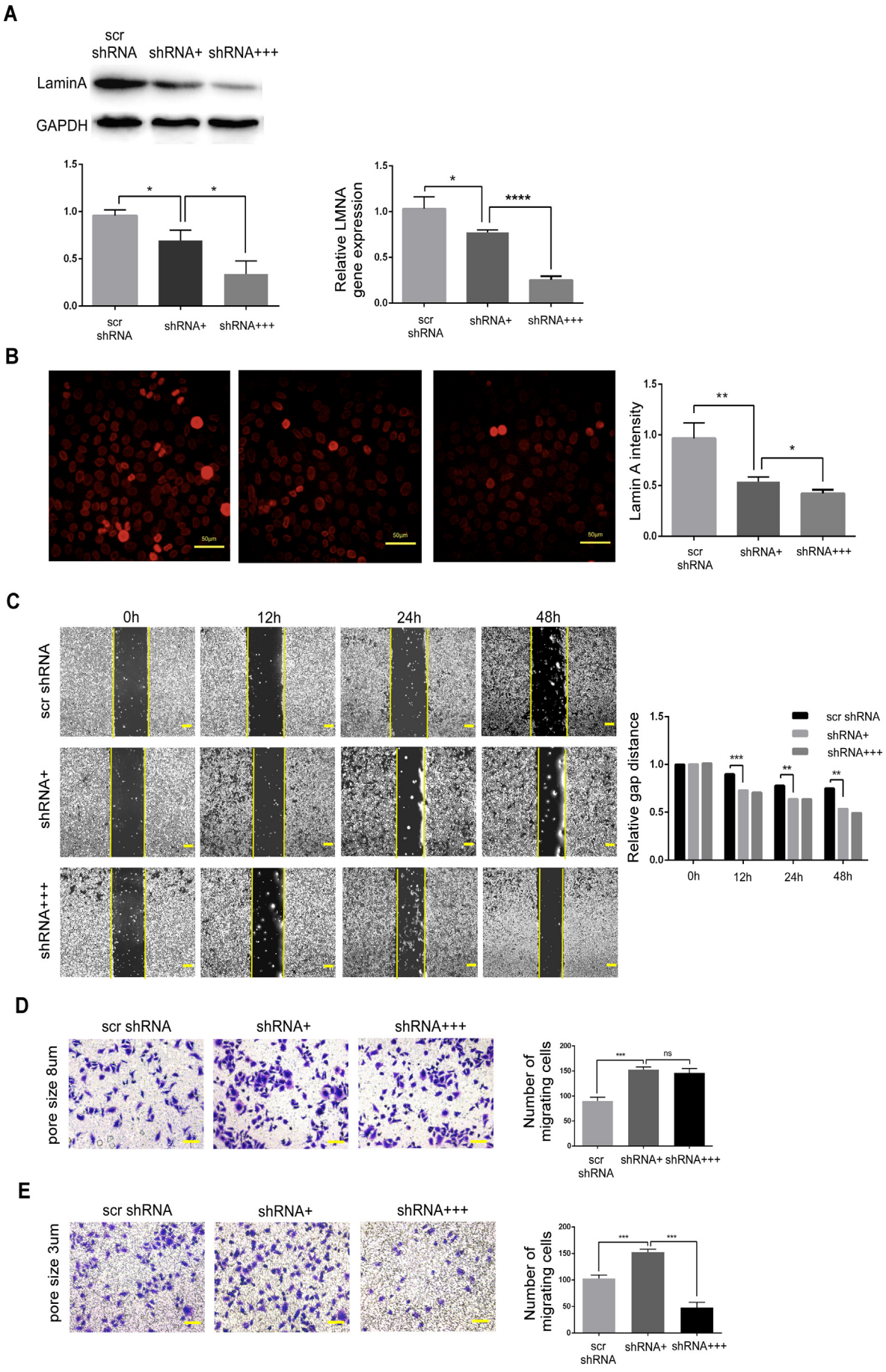
A
scr shRNA
shRNA+
shRNA+++
LaminA
GAPDH
Relative LMNA gene expression
B
Lamin A intensity
C
0h
12h
24h
48h
scr shRNA
shRNA+
shRNA+++
Relative gap distance
D
pore size 8um
Number of migrating cells
ns
E
pore size 3um

Results showed that the expressions of BRCA1, Ku80 and Rad50 did not change obviously after lamin-A moderate knockdown (Fig. 3E), but were down-regulated significantly after further knockdown (Fig. 3E, $p < 0.01$), suggesting impairment of both NHEJ and HR pathways in DNA damage repair.

Overexpression of lamin-A impeded the migration ability of ovarian cancer cells.

Different from HO-8910, HO-8910PM has relative low expression of lamin-A. When transfected with flag-lamin-A, lamin-A was significantly up-regulated to 24 fold by qRT-PCR, and western blot showed the same trend (Fig. 4A, $p < 0.001$). Then, wound healing assay (2D), transwell assay (3D) were used to assess the effect of lamin-A overexpression on migration of HO-8910PM cells. After treatment with flag-lamin-A, 2D migration was significantly inhibited (Fig. 4B). Then the two groups were transferred through relative large pores (8 μm, Fig. 4C) as well as constricted pores (3 μm, Fig. 4D), and discovered that overexpression of lamin-A strongly impeded the 3D migration of HO-8910PM cells with statistically significant difference ($p < 0.001$).

Lamin-A overexpression influenced the nuclear morphology, DNA damage, and micronuclei formation after migrated through constricted pores.

HO-8910PM cells transfected with flag-lamin-A or control vector were migrated through relatively large pores (8 μm). Immunofluorescence showed the nuclei appeared to be similar in shape on top and bottom. However, when migration was carried out through constricted pores (3 μm), nuclear shapes on the bottom of the filters were elongated compared with the typical elliptical shapes on the top surface in lamin-A overexpression group, and the circularity of nuclei increased in control (Fig. 5A, $p < 0.05$), indicating that the nuclear morphology after restricted migration was related to the level of lamin-A. In addition, micronuclei with γ-H2AX staining were also observed in HO-8910 PM cells (Fig. 5B). Besides, when cells migrated through restricted pores, γ-H2AX positive rate decreased after overexpression of lamin-A (Fig. 5C, $p < 0.001$), whereas no significant difference between the two groups was found for 8 μm pores (Fig. 5D).

Nuclear morphology was affected after lamin-A further knockdown detected by transmission electron microscopy.

To further detect the changes of nuclear shape, and achieve higher spatial resolution of nuclei, shRNA+++ treated group and the control were subjected to transmission electron microscopy (TEM) analyses. Control cells showed intact nuclei, which appeared smooth with oval shape and normal chromatin distribution (Fig. 6A). But after further knockdown of lamin-A, distorted nucleus with nuclear incisures appeared, and sometimes with a micronucleus next to it (Fig. 6B, arrow). In addition, TEM also showed that different from a typical nuclear structure, chromatin dissolution was observed in some of the nuclei, with loosely arranged chromatin (Fig. 6C, arrow). Besides, nuclear protrusions could also be seen in some of the nuclei (Fig. 6C, arrowhead).

5. Discussion

The nuclear envelope (NE) consists of the inner nuclear membranes (INM) and outer nuclear membranes (ONM), INM and ONM are different in function, and are connected through nuclear pores [18,19]. Nuclear lamina is located below the INM, and is required in maintaining nuclear structure and integrity. It also plays an important role in a series of cell processes, such as regulation of gene expression, DNA replication and repair, apoptosis, senescence and chromatin organization [20]. Besides, researchers also found that lamina was essential in the nuclear morphology, related to the size, shape and mechanical stability of the nucleus [21,22].

Lamin-A is encoded by LMNA gene. The expression of lamin-A could change in many diseases. Recent studies have shown that lamin-A was down-regulated in tumor cells [23,24], but also could be up-regulated sometimes [23,25,26], so the expression and function of lamin-A were particularly complex. The GEPIA online database revealed that lamin-A levels tended to be lower in many kinds of cancers including ovarian cancer (Fig. 1A). In our previous study, immunohistochemistry demonstrated that lamin-A was lower in ovarian cancer tissues than that in normal ovarian tissues. These were further confirmed by the data from GEO database (Fig. 1D). Besides, Kaplan-Meier curves of OS (survival rate) and PFS (progression-free survival rate) further verified that low lamin-A expression was significantly associated with poorer survival in ovarian cancer patients, whereas high lamin-A level was associated with better prognosis (Fig. 1B, C). Next, the effect of lamin-A on migration of ovarian cancer cells was investigated. In our study, the 2D and 3D migration abilities of HO-8910 cells enhanced after lamin-A moderate knockdown (Fig. 2, Supplementary Fig. S1), with no obvious changes of the nuclear shape (Fig. 3A), whereas overexpression of lamin-A in HO-8910 PM cells led to a decline in cell migration (Fig. 4). This indicated that the expression level of lamin-A was critical for cell migration, down-regulation of lamin-A could decrease the hardness of cells and enhance the ability of migrating through transwell filters [27,28]. Surprisingly, cells showed a biphasic dependence on lamin-A levels in migration through 3 μm filters. Relative to scrambled shRNA treated cells, moderate knockdown group (denoted as shRNA+) produced the greatest increase in 3D migration (Fig. 2E), but knockdown level had no effect on 2D migration and migration through 8 μm pores (Fig. 2C, D), which were approximately sevenfold larger than the smaller pores, and required much less distortion of nuclei. In addition, we noticed that differences in the morphology of nuclei appeared on the bottom of the 3 μm pores, cells with relative high lamin-A had elongated nuclear shapes (Fig. 3A), and the circularity of nuclei increased with the decrease of lamin-A (Figs. 3A,5A). However, for 8 μm pores, lamin-A knockdown had no effect on shapes of nuclei on the filter bottoms. These results indicated that nuclei with high lamin-A were severely deformed and difficult to recover during migration through constricted pores, suggesting that lamin-A was essential in the mechanical stability of the nucleus [29,30], especially in maintaining the oval shape [29]. The down-regulation of lamin-A could enhance the plasticity of the nucleus, making the cells more prone to deformation through restrictive pores, and the morphology was easier to recover. Besides, constricted migration increased the positive rate of γ-H2AX foci especially in the lamin-A further knockdown group (Fig. 3B), indicating formation of DSBs and lethal DNA damage [31], which, if not repaired, could lead to cell death [32,33]. Furthermore, micronuclei were observed in some cells after lamin-A further knockdown (Fig. 3C). Micronuclei are satellite nuclei, often γ-H2AX positive, with roles in genome remodeling. Micronucleus formation is the result of many cell division defects, including mitotic errors, DNA replication or repair errors [34,35], making the complete chromosome segment into micronucleus [36]. As shown in the TEM, distorted nuclei with micronuclei or nuclear protrusions could be found in lamin-A further knockdown group (Fig. 6B, C).

In summary, DNA damage was easy to happen in cells passing through constricted pores, and the damage was more serious with the

Fig. 2. Further knockdown of lamin-A impeded migration capacity of ovarian cancer cells through restricted pores A: Knockdown efficiency was determined by western blot and qRT-PCR. B: Representative images of cells stained for lamin-A and quantitative results of lamin-A intensity. HO-8910 cells were transfected with shRNA+, shRNA+++, and scrambled vector as control. Scale bars, 50 μm. C: Representative images and quantitative results of wound-healing assay. HO-8910 cells were transfected with shRNA+, shRNA+++, and scrambled vector as control. Scale bars, 100 μm. D: Cell migration was determined by transwell assay. HO-8910 cells were transfected with scrambled control or shRNA+, shRNA+++. Quantitative results were shown (8 μm). Scale bars, 50 μm. E: Cell migration was determined by transwell assay. HO-8910 cells were transfected with scrambled control or shRNA+, shRNA+++. Quantitative results were shown (3 μm). Scale bars, 50 μm. All the experiments were repeated three times. All the error bars indicated means ± SD. Statistical significance was concluded at $^{*}p < 0.05$; $^{**}p < 0.01$; $^{***}p < 0.001$.

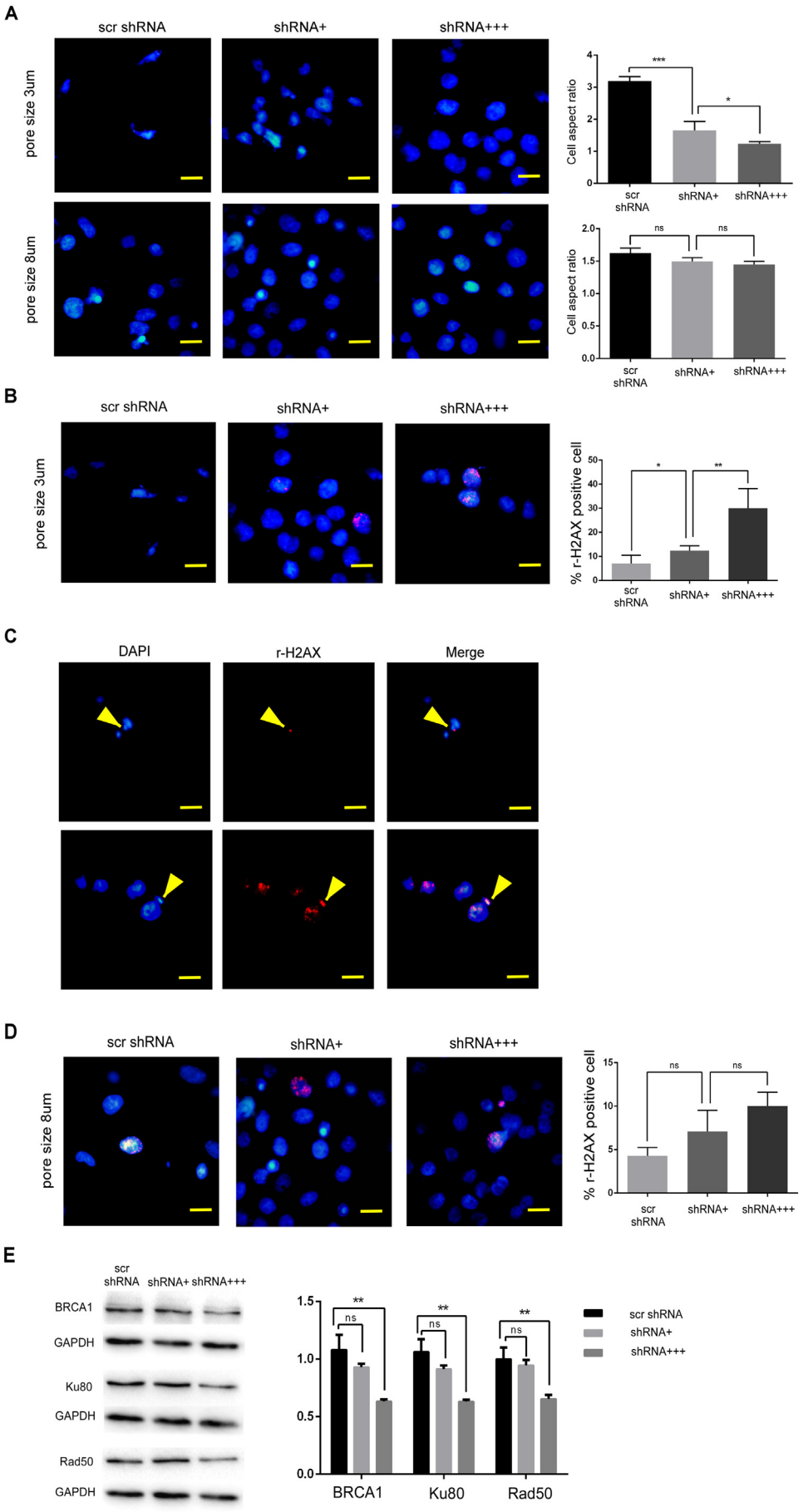
A
scr shRNA
shRNA+
shRNA+++
pore size 3um
pore size 8um
Cell aspect ratio
***
*
ns
ns
scr shRNA
shRNA+
shRNA+++
B
% r-H2AX positive cell
C
DAPI
r-H2AX
Merge
D
E
BRCA1
GAPDH
Ku80
Rad50
**

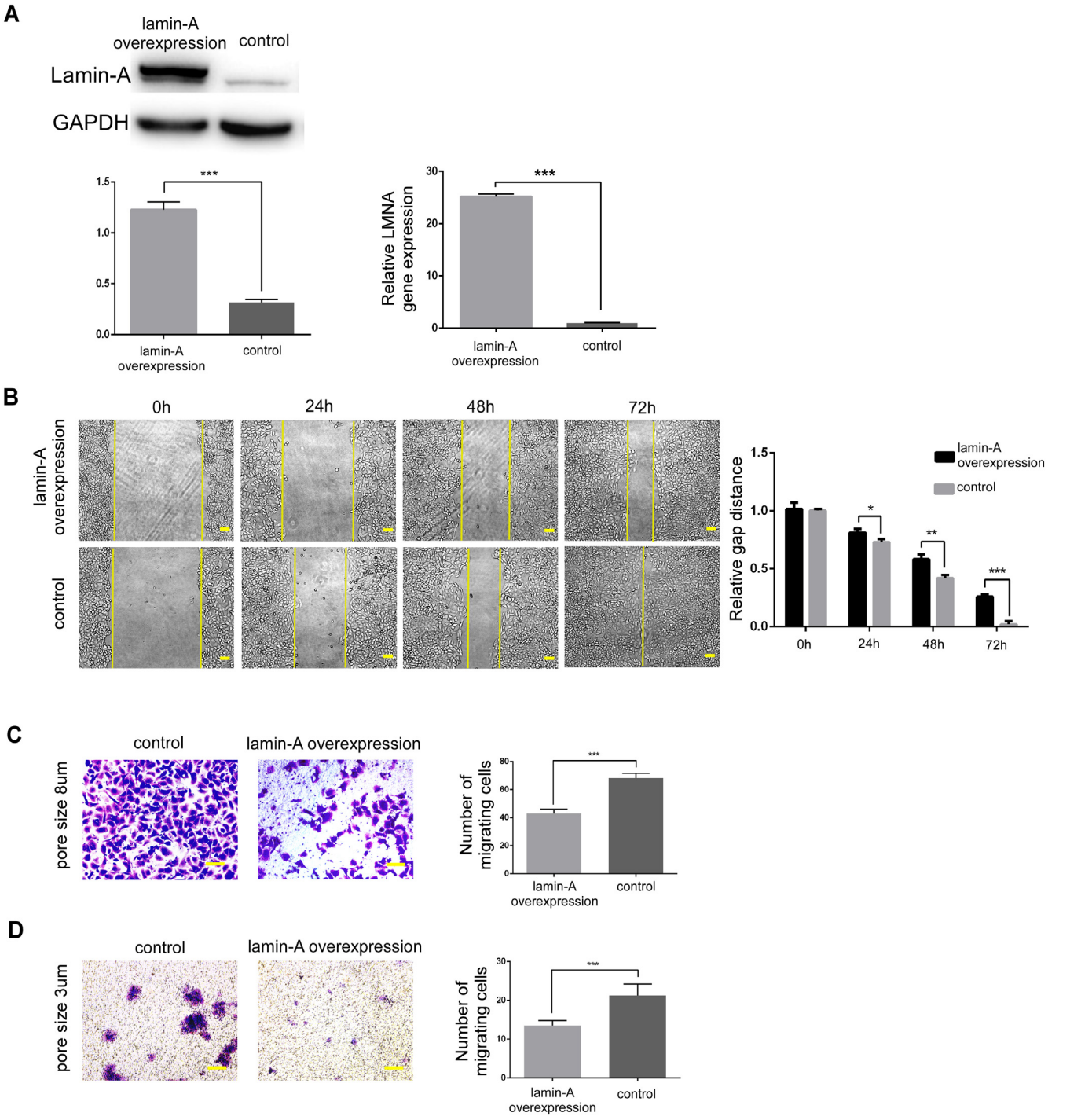

Fig. 4. Overexpression of lamin-A impeded the migration ability of ovarian cancer cells A: Overexpression was determined by western blot and qRT-PCR. B: Representative images and quantitative results of wound-healing assay. HO-8910PM cells were transfected with flag-lamin-A, and scrambled vector as control. Scale bars, 100 μm. C: Cell migration was determined by transwell assay. HO-8910PM cells were transfected with scrambled control or flag-lamin-A. Number of migrating cells was shown (8 μm). Scale bars, 50 μm. D: Cell migration was determined by transwell assay. HO-8910 PM cells were transfected with scrambled control or flag-laimin-A. Number of migrating cells was shown (3 μm). Scale bars, 50 μm. All the experiments were repeated three times. All the error bars indicated means ± SD. Statistical significance was concluded at $^{*}p < 0.05$; $^{**}p < 0.01$; $^{***}p < 0.001$.

decrease of lamin-A and even caused genomic instability after restricted migration. Furthermore, we also studied the possible mechanism of this phenomenon. DSBs could be repaired by NHEJ and HR [37,38], of which BRCA1, Ku80, and Rad50 are the key proteins of the repair pathways. Western blot showed that their expression decreased significantly after lamin-A further knockdown (Fig. 3E), suggesting impairment of

Fig. 3. Lamin-A knockdown influenced the nuclear morphology, DNA damage, and micronuclei formation after migrated through constricted pores A: Nuclei on the bottom of the filters stained for DNA (DAPI, blue) after migrated through 3 μm and 8 μm pores. Scale bars, 20 μm. B: Representative images of γ-H2AX foci and quantitative results of γ-H2AX positive cells (3 μm). Scale bars, 20 μm. C: Representative images of micronuclei (arrows) stained for γ-H2AX (red) and DNA (DAPI, blue). Scale bars, 20 μm. D: Representative images of γ-H2AX foci and quantitative results of γ-H2AX positive cells (8 μm). Scale bars, 20 μm. E: The protein levels of BRCA1, Ku80 and Rad50 were measured by western blot after lamin-A moderate and further knockdown, GAPDH was used as the endogenous reference protein. All the experiments were repeated three times. All the error bars indicated means ± SD. Statistical significance was concluded at $^{*}p < 0.05$; $^{**}p < 0.01$; $^{***}p < 0.001$.

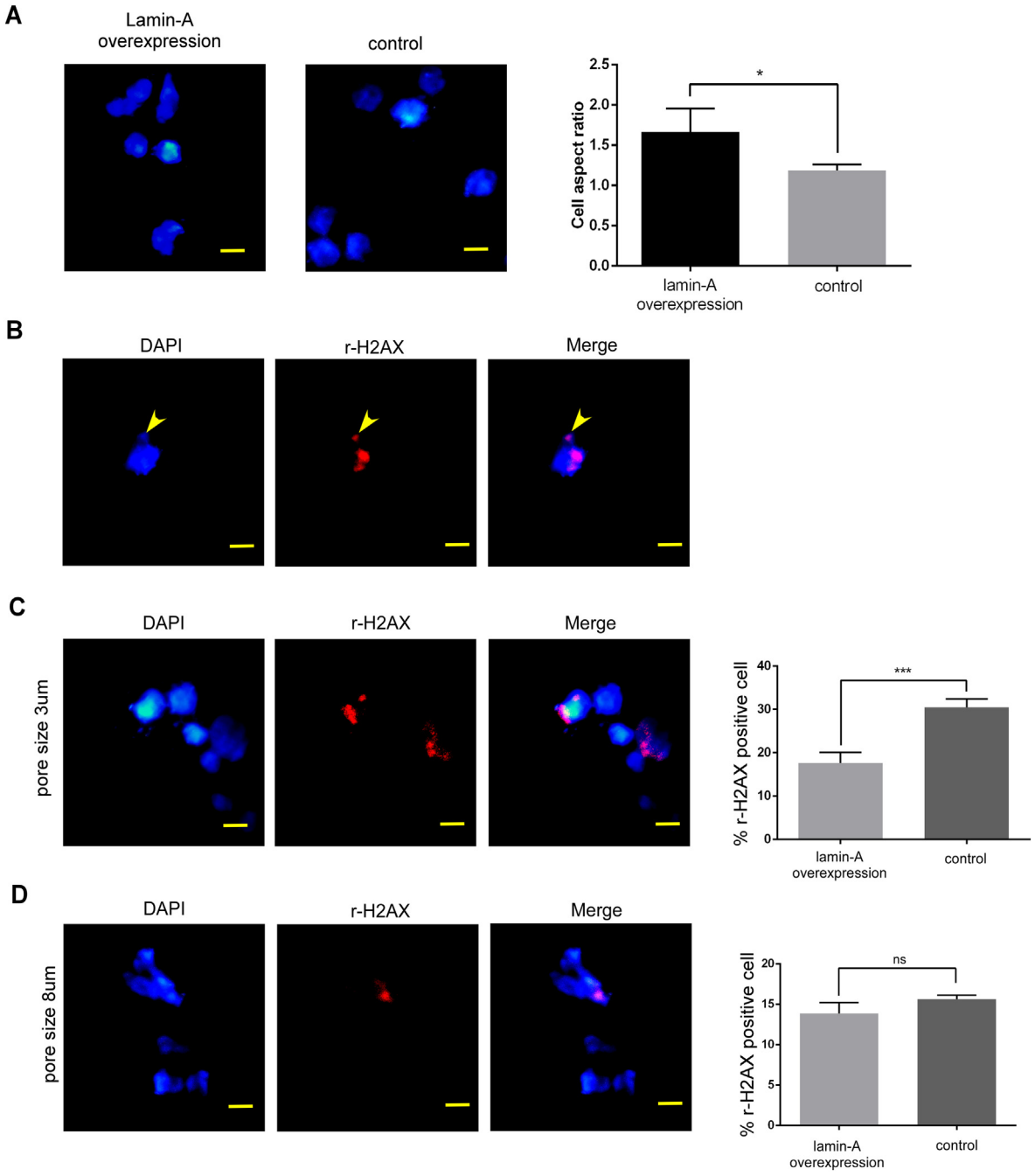

Fig. 5. Lamin-A overexpression influenced the nuclear morphology, DNA damage, and micronuclei formation after migrated through constricted pores A: Nuclei on the bottom of the filters stained for DNA (DAPI, blue) after migrated through 3 μm pores. Scale bars, 20 μm. B: Representative images of micronucleus (arrows) stained for γ-H2AX (red) and DNA (DAPI, blue). Scale bars, 20 μm. C: Representative images of γ-H2AX foci and quantitative results of γ-H2AX positive cells (3 μm). Scale bars, 20 μm. D: Representative images of γ-H2AX foci and quantitative results of γ-H2AX positive cells (8 μm). Scale bars, 20 μm. All the experiments were repeated three times. All the error bars indicated means ± SD. Statistical significance was concluded at $^{*}p < 0.05$; $^{***}p < 0.001$.

both NHEJ and HR. Normally, Rad50 could rapidly localized at the site of DSBs to recruit other DNA repair proteins such as Ku80, BRCA1 and so on [39,40]. Once lamin-A was further knockdown, the repair pathways were damaged. When cells passed through 3 μm filters, which required more distortion of nuclei and caused more DNA damage, cells may not express and recruit adequate DNA repair proteins, and may not initiate DNA repair in time. Therefore, we considered that these might be account for the decrease of cell number after constricted migration in lamin-A further knockdown group, as well as chromosome breakage and micronuclei formation, which indicated genomic instability. This would be further investigated in our following research.

Supplementary data to this article can be found online at https://doi.org/10.1016/j.ygyno.2018.10.030.

Conflict of interest

The authors have declared that no competing interest exists.

Author contribution

Yixuan Wang and Xiaoying Wu designed the study; Yixuan Wang analyzed the data with contributions from Liuqing He; Yixuan Wang

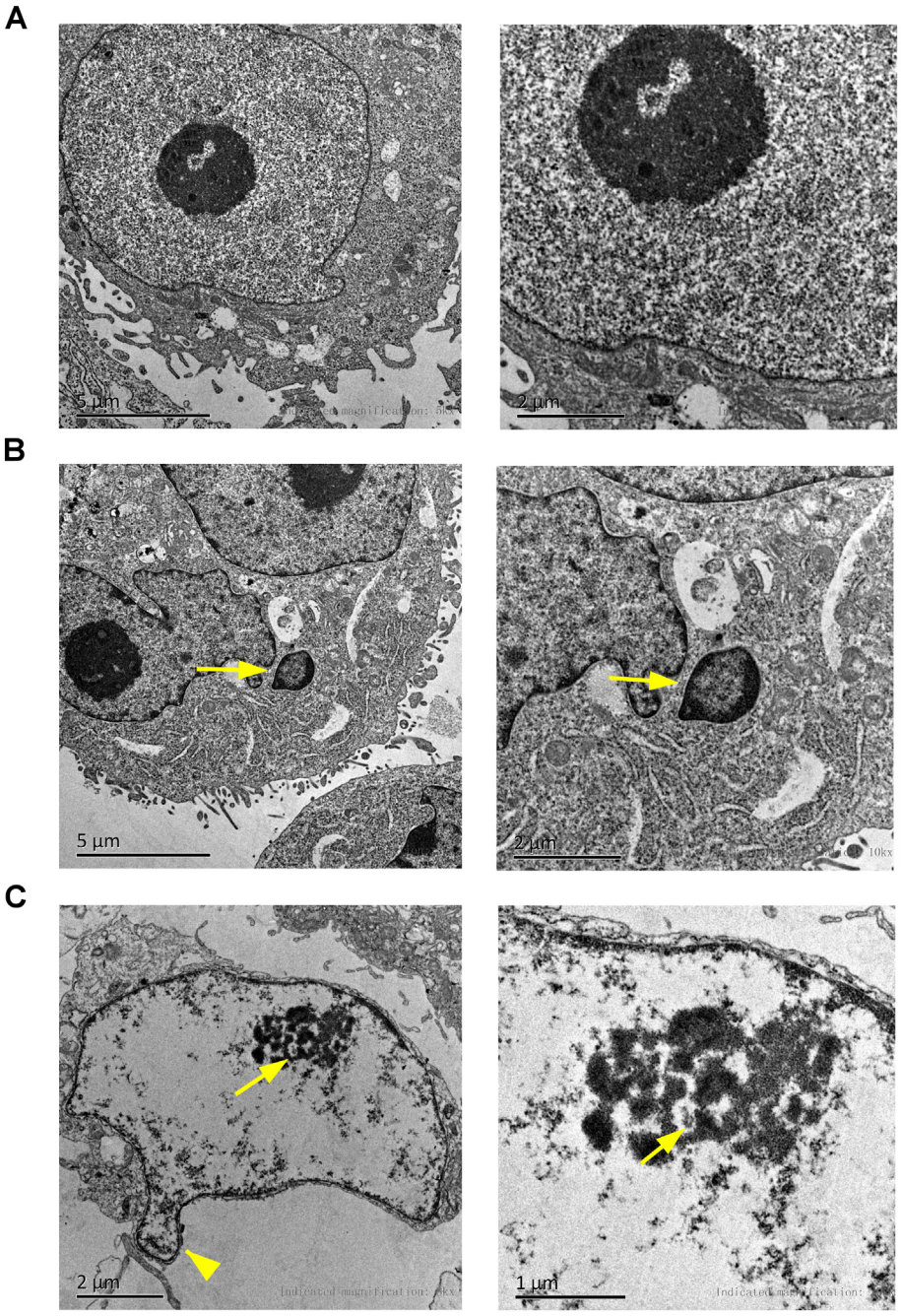

Fig. 6. Nuclear morphology was affected after Lamin-A further knockdown detected by transmission electron microscopy A: TEM images of control HO-8910 nucleus, with regular nuclear shape and chromatin distribution. B: TEM images of cells treated with shRNA+++. Abnormal nuclear morphology was found with incisure and micronucleus (arrows). C: TEM images of cells treated with shRNA+++. Abnormal nuclear morphology was found with chromatin dissolution and nuclear protrusion (arrowhead).

performed the experiments, with contributions from Jing Jiang and Guanghui Gong; Yixuan Wang wrote the manuscript.

References

[1] S.R. Schulze, B. Curio-Penny, S. Speese, et al., A comparative study of Drosophila and human A-type lamins, PLoS One 4 (2009) 7564.
[2] T. Dechat, K. Pfleghaar, K. Sengupta, et al., Nuclear lamins: major factors in the structural organization and function of the nucleus and chromatin, Genes Dev. 22 (2008) 832–853.
[3] N.M. Maraldi, C. Capanni, V. Cenni, et al., Laminopathies and lamin-associated signaling pathways, J. Cell. Biochem. 112 (2011) 979–992.
[4] A. Mattout, T. Dechat, S.A. Adam, et al., Nuclear lamins, diseases and aging, Curr. Opin. Cell Biol. 18 (2006) 335–341.
[5] Z. Wu, L. Wu, D. Weng, et al., Reduced expression of lamin A/C correlates with poor histological differentiation and prognosis in primary gastric carcinoma, J. Exp. Clin. Cancer Res. 28 (2009) 8.
[6] E.J. Belt, R.J. Fijneman, E.G. van den Berg, et al., Loss of lamin A/C expression in stage II and III colon cancer is associated with disease recurrence, Eur. J. Cancer 47 (2011) 1837–1845.
[7] C.D. Capo-chichi, K.Q. Cai, J. Smedberg, et al., Loss of A-type lamin expression compromises nuclear envelope integrity in breast cancer, Chin. J. Cancer 30 (2011) 415–425.
[8] C.D. Capo-chichi, K.Q. Cai, F. Simpkims, et al., Nuclear envelope structural defects cause chromosomal numerical instability and aneuploidy in ovarian cancer, BMC Med. 9 (2011) 28.
[9] N.D. Willis, R.G. Wilson, C.J. Hutchison, et al., Lamin A: a putative colonic epithelial stem cell biomarker which identifies colorectal tumors with a more aggressive phenotype, Biochem. Soc. Trans. 36 (2008) 1350–1353.
[10] J. Li, L. Li, Z. Li, et al., The role of miR-205 in the VEGF-mediated promotion of human ovarian cancer cell invasion, Gynecol. Oncol. 137 (2015) 125–133.

[11] G. Gong, P. Chen, L. Li, et al., Loss of lamin A but not lamin C expression in epithelial ovarian cancer cells is associated with metastasis and poor prognosis, Pathol. Res. Pract. 211 (2015) 175–182.
[12] Z. Tang, C. Li, B. Kang, G. Gao, C. Li, Z. Zhang, GEPIA: a web server for cancer and normal gene expression profiling and interactive analyses, Nucleic Acids Res. 45 (W1) (2017) W98-102, https://doi.org/10.1093/nar/gkx247.
[13] T.L1. Yeung, C.S. Leung, K.K. Wong, et al., TGF-β modulates ovarian cancer invasion by upregulating CAF-derived versican in the tumor microenvironment, Cancer Res. 73 (16) (2013 Aug 15) 5016–5028.
[14] Matsumura N1, Z. Huang, S. Mori, et al., Epigenetic suppression of the TGF-beta pathway revealed by transcriptome profiling in ovarian cancer, Genome Res. 21 (1) (2011 Jan) 74–82.
[15] Yoshihara K1, A. Tajima, D. Komata, et al., Gene expression profiling of advanced-stage serous ovarian cancers distinguishes novel subclasses and implicates ZEB2 in tumor progression and prognosis, Cancer Sci. 100 (8) (2009 Aug) 1421–1428.
[16] E.R1. King, C.S. Tung, Y.T. Tsang, et al., The anterior gradient homolog 3 (AGR3) gene is associated with differentiation and survival in ovarian cancer, Am. J. Surg. Pathol. 35 (6) (2011 Jun) 904–912.
[17] B. Gyorffy, A. Lanczky, Z. Szallasi, Implementing an online tool for genome-wide validation of survival-associated biomarkers in ovarian-cancer using microarray data of 1287 patients, Endocr. Relat. Cancer 19 (2) (2012 Apr 10) 197–208.
[18] R. Foisner, Inner nuclear membrane proteins and the nuclear lamina, J. Cell Sci. 114 (2001) 3791–3792.
[19] P. Jevtić, L.J. Edens, L.D. Vuković, et al., Sizing and shaping the nucleus: mechanisms and significance, Curr. Opin. Cell Biol. 28 (2014) 16–27.
[20] J.L. Broers, F.C. Ramaekers, G. Bonne, et al., Nuclear lamins: laminopathies and their role in premature ageing, Physiol. Rev. 86 (2006) 967–1008.
[21] A.D. Waters, A. Bommakanti, O. Cohen-Fix, Shaping the nucleus: factors and forces, J. Cell. Biochem. 113 (2012) 2813–2821.
[22] P. Jevtić, L.J. Edens, X. Li, et al., Concentration-dependent effects of nuclear lamins on nuclear size in *Xenopus* and mammalian cells, J. Biol. Chem. 290 (2015) 27557–27571.
[23] J.L. Broers, Y. Raymond, M.K. Rot, et al., Nuclear A-type lamins are differentially expressed in human lung cancer subtypes, Am. J. Pathol. 143 (1993) 211–220.
[24] S.F. Moss, V. Krivosheyev, A. de Souza, et al., Decreased and aberrant nuclear Lamin expression in gastrointestinal tract neoplasms, Gut 45 (1999) 723–729.
[25] C.M. Tilli, F.C. Ramaekers, J.L. Broers, et al., Lamin expression in normal human skin, actinic keratosis, squamous cell carcinoma and basal cell carcinoma, Br. J. Dermatol. 148 (2003) 102–109.
[26] M.E. Hudson, I. Pozdnyakova, K. Haines, et al., Identification of differentially expressed proteins in ovarian cancer using high-density protein microarrays, Proc. Natl. Acad. Sci. U. S. A. 104 (2007) 17494–17499.
[27] J.W. Shin, K.R. Spinler, J. Swift, et al., Lamins regulate cell trafficking and lineage maturation of adult human hematopoietic cells, Proc. Natl. Acad. Sci. U. S. A. 110 (2013) 18892–18897.
[28] T. Harada, J. Swift, J. Irianto, et al., Nuclear lamin stiffness is a barrier to 3D migration, but softness can limit survival, J. Cell Biol. 204 (2014) 669–682.
[29] J. Lammerding, L.G. Fong, J.Y. Ji, et al., Lamins A and C but not lamin B1 regulate nuclear mechanics, J. Biol. Chem. 281 (2006) 25768–25780.
[30] J.D. Pajerowski, K.N. Dahl, F.L. Zhong, et al., Physical plasticity of the nucleus in stem cell differentiation, Proc. Natl. Acad. Sci. U. S. A. 104 (2007) 15619–15624.
[31] J.P. Banath, D. Klokov, S.H. MacPhail, et al., Residual gammaH2AX foci as an indication of lethal DNA lesions, BMC Cancer 10 (2010) 4.
[32] B. Ewald, D. Sampath, W. Plunkett, Nucleoside analogs: molecular mechanisms signaling cell death, Oncogene 27 (2008) 6522–6537.
[33] M.T. Tomicic, B. Kaina, Topoisomerase degradation, DSB repair, p53 and IAPs in cancer cell resistance to camptothecin-like topoisomerase I inhibitors, Biochim. Biophys. Acta 1835 (2013) 11–27.
[34] M. Terradas, M. Martin, L. Tusell, et al., Genetic activities in micronuclei: is the DNA entrapped in micronuclei lost for the cell? Mutat. Res. 705 (2010) 60–67.
[35] D.R. Hoffelder, L. Luo, N.A. Burke, et al., Resolution of anaphase bridges in cancer cells, Chromosoma 112 (2004) 389–397.
[36] K. Crasta, N.J. Ganem, R. Dagher, et al., DNA breaks and chromosome pulverization from errors in mitosis, Nature 482 (2012) 53–58.
[37] M. Shrivastav, L.P. De Haro, J.A. Nickoloff, Regulation of DNA double-strand break repair pathway choice, Cell Res. 18 (2008) 134–147.
[38] E. Sonoda, H. Hochegger, A. Saberi, et al., Differential usage of non-homologous end-joining and homologous recombination in double strand break repair, DNA Repair (Amst) 5 (2006) 1021–1029.
[39] T.T. Paull, E.P. Rogakou, V. Yamazaki, et al., A critical role for histone H2AX in recruitment of repair factors to nuclear foci after DNA damage, Curr. Biol. 10 (2000) 886–895.
[40] M.F. Lavin, S. Kozlov, M. Gatei, et al., ATM-dependent phosphorylation of all three members of the mrn complex: from sensor to adaptor, Biomol. Ther. 5 (2015) 2877–2902.